Properties of Pulsed Current Multipass GMA-Welded Al-Zn-Mg Alloy

Pulsed current multipass GMA welding of thick Al-Zn-Mg alloy section improves the fatigue life of the weld compared to the welds produced by continuous current GMA welding

BY H. M. HUSSAIN, P. K. GHOSH, P. C. GUPTA AND N. B. POTLURI

ABSTRACT. Multipass pulse and continuous current GMA welding of a 25-mm-thick extruded section of Al-Zn-Mg alloy 7005 was carried out using Al-Mg 5183 filler metal. During welding, the pulse parameters, such as the pulse frequency and duration, were varied and their effect on dilution, zinc pickup, precipitation behavior, microstructure refinement, porosity content and fatigue life (N) of the weld were studied. It was observed that the variation in the pulse parameters affects the dilution, zinc pickup, porosity content, amount of precipitate and microstructure refinement of the weld. The ultimate tensile strength and fatigue life of the weld joints are found to vary with the pulse parameters. The zinc pickup, finer dendrite fraction, porosity content and tensile strength of the weld are correlated to its fatigue life. The characteristics and fatigue life of the pulsed current weld are compared to those of the continuous current weld. The increase in zinc pickup and finer dendrite fraction of the weld enhances the fatigue life of the weld joints; whereas, the increase in porosity content to 3.4 vol-% adversely affects the same. At certain pulse parameters, the fatigue life of the weld joints is markedly improved over that of the continuous current weld joints.

H. M. HUSSAIN, P. K. GHOSH and P. C. GUPTA are with Welding Research Laboratory, Department of Mechanical and Industrial Engineering, University of Roorkee, Roorkee, India. N. B. Potluri is with the Materials Engineering Program, Auburn University, Auburn, Ala.

Introduction

The Al-Zn-Mg alloy has gathered wide acceptance in the fabrication of lightweight structures requiring a high strength-to-weight ratio, such as transportable bridge girders, road tankers and railway transport systems (Refs. 1, 2). In any structural application of this alloy consideration of its weldability is of utmost importance as welding is largely used for joining of structural components. Due to the application of this alloy in high-strength structures, it is imperative to characterize the fatigue properties of the weld along with its tensile properties, especially when the fatigue properties of high-strength aluminum alloys are having a complex pattern of interaction with the mechanical properties and microstructure of the matrix.

The preferred welding process of Al-Zn-Mg alloy is frequently gas metal arc (GMA) due to its comparatively easier applicability and better economy (Ref. 3). In the case of single-pass GMA welding of thinner section (≤ 10 mm) of this alloy, the pulsed current has been found beneficial due to its advantages over the conventional continuous current process, such as better control on metal deposition (Refs. 4,5) and weld thermal cycle (Ref. 6). In most of the weldments of Al-Zn-Mg alloy, the fracture has been found to take place in the weld region (Ref. 7–12) under static and dynamic loading. However, the use of pulsed current GMA welding has been found to improve the tensile strength and fatigue life of the weld compared to those of conventional continuous current GMA welds of this alloy (Refs. 7–9, 11, 12). The change in tensile and fatigue properties of the weld is found to be largely affected by the weld characteristics, such as microstructure, chemical composition and porosity content of the weld, which are governed by the pulse parameters (Refs. 9, 11–16).

Key Words

Pulsed GMAW
Continuous Current
Multipass
Al-Zn-Mg
Zinc Pickup
Microstructure
Porosity
Pulse Parameters
Fatigue Life

The increasing demand for using comparatively thicker sections of aluminum alloys in several fields, such as pressure vessels, structural columns and transport systems (Ref. 17), necessitates multipass welding for joining of those sections. In multipass welding, the weld characteristics, and consequently its mechanical properties, differ from those observed in the case of single-pass welds. However, hardly any systematic study has been reported so far showing the characteristics and fatigue properties of a multipass pulsed current GMA weld of comparatively thicker sections of Al-Zn-Mg alloy.

In this investigation, an effort has been made to study at a given mean current the influence of pulse parameters, namely: pulse frequency, pulse duration and pulse off time fraction on the fatigue properties of a multipass Al-Zn-Mg alloy weld. The fatigue life has been correlated

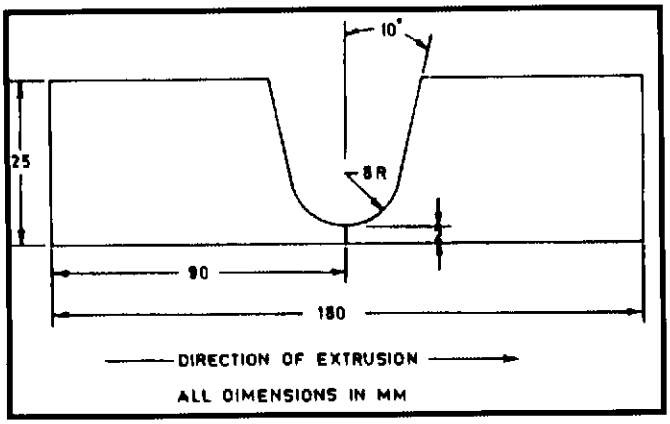

Fig. 1 — Schematic diagram of the weld groove.

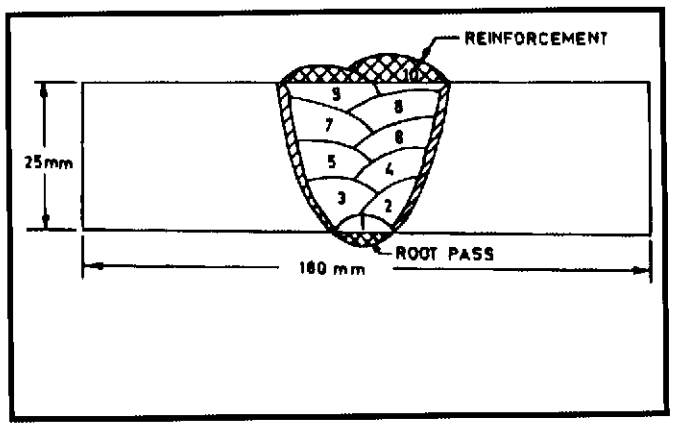

Fig. 2 — Schematic diagram of the sequence of weld passes.

with the microstructure, zinc pickup, porosity content, and tensile strength of the weld. Finally, the properties of the weldments prepared by multipass pulsed current GMA welding are compared with those of the multipass weldments prepared by coventional continuous current GMA welding.

Experimental Procedure

Pulsed current GMA welding of an extruded section (40 x 25 mm) of Al-Zn-Mg alloy (7005) was carried out using 1.6-mm-diameter filler metal (5183) and commercial argon (99.98%) as shielding gas at a flow rate of 20 L/min. The welding was carried out by filling the weld groove (Fig. 1) in ten passes — Fig. 2. Prior to welding, the plates were thoroughly cleaned to remove the oxide layer and any dirt or grease adhering to the groove surface. The pulsed current welding was carried out at a given mean current of 220 A where the pulse frequency and pulse duration were varied in the range of 25–100 Hz at 4.5–8.5 ms, respectively — Table 1. The mean current was selected on the hasis of earlier observations (Refs. 6–13) that showed its effectiveness in improving weld properties. Before welding, a number of pieces were placed side by side, so their grooves were properly aligned for each weld pass and rigidly held in a fixture to minimize distortion during welding. The welding was carried out on a stainless steel backing plate to obtain uniform root penetration. Both the preheat and interpass temperatures were maintained as 393 K. During the deposition of the fill passes adjacent to the groove edge, a clearance of about 1.5 mm was maintained between the electrode and the groove edge to ensure proper fusion of the base metal. Between subsequent fill passes, the surface of the earlier deposit was thoroughly cleaned using a stainless steel wire brush. For a comparative study, the welds were also produced with conventional continuous current (without pulse) GMA welding process using the same welding current as that of the mean current used in the pulsed current welding. The arc voltage and welding speed were kept constant as 23 V and 300 mm/min, respectively. During welding the pulse characteristics were recorded with an oscilloscope. The peak current (I_p), pulse duration (t_p) and pulse off time (t_b) were estimated (Table 1) with the help of a digital oscilloscope; whereas, the mean (I_m) and base (I_b) currents were recorded from an ammeter fixed in the welding power source.

Table 1 — Welding Parameters

Specimen Designation	Mean Welding Current (A)	Pulse Frequency (Hz)	Pulse Duration (ms)	Pulse off time Fraction	Base Current (A)	Peak Current (A)
A	220	0	0	—	—	—
B	220	25	4.5	0.8875	190	373
C	220	50	4.5	0.775	160	366
D	220	100	4.5	0.55	110	352
E	220	25	6.5	0.8375	160	438
F	220	50	6.5	0.675	120	421
G	220	100	6.5	0.35	60	361
H	220	25	8.5	0.7875	150	455
I	220	50	8.5	0.575	110	424
J	220	100	8.5	0.15	50	376

Before collecting specimens for testing, the weldments were stored at room temperature (295 K) for more than 30 days so they would naturally age sufficiently. The weld reinforcement of both the top and bottom surfaces of the weldments was machined flat. The presence of zinc in the weld deposit and the detailed chemical composition of the base and filler metals were analyzed under an atomic absorption spectrometer.

Specimens for metallographic examination were cut from the central part of the weldment to ensure a true representation of the weld characteristics. Transverse sections of the specimens were prepared by standard metallographic technique and suitably etched in Keller's reagent to reveal the microstructure. The microstructure of the weld was studied both under optical and scanning electron microscopes. The quantification of the coarse and fine dendritic portions of the matrix was carried out by the standard lineal intercept method (Ref. 18). An x-ray diffraction study of the powder collected from the weld metal was carried out to determine the presence of any intermetallic precipitate. Porosity content of the weld (excluding reinforcement), revealed as dark spots on the metallographically polished and unetched transverse section of the weld, was estimated under the optical microscope following the standard point counting method (Ref. 18).

A tensile test of the weld joint was performed with a Servo Hydraulic Universal Testing Machine using round tensile specimens (DIN 50215), which had weld metal at their centers as shown in Fig. 3. Tensile properties of the base metal were also determined using the similar round tensile specimen. The tensile test was carried out at a cross head speed of 1 mm/min. Yield strength was determined at 0.2% offset strain on the

load vs. strain diagram obtained with an extensometer fixed on the gauge length portion (50 mm) of the specimen. The elongation of the joint was also estimated over the same gauge length.

Fatigue life (N cycle) of the weldments was studied using three specimens from each welding parameter. The specimens, having a cross-sectional area of 12.5 x 7 mm and gauge length of 50 mm with the weld at its center (Fig. 4), were tested according to the ASTM (E466-82) standard (Ref. 19). Tests were carried out under uniaxial loading on a hydraulically operated pulsator operated at a mean stress of 80 N/mm^2, a stress ratio (minimum stress/maximum stress) R of 0.5, and a stress cycle of 5 Hz. The number of cycles to fracture was recorded.

Results and Discussion

Chemical analysis

The chemical composition of the base and filler metals is shown in Table 2. The table shows that the filler metal does not contain zinc but the base material has a considerable amount of zinc in it. The selection of (Al-Mg) filler metal containing no zinc was made as per recommended practice (Ref. 20), where the weld deposit provides good mechanical properties and corrosion resistance. However, the weld deposit has been found to pick up zinc from the base metal due to dilution (Table 3).The influence of pulse frequency duration and off time fraction ($t_p/(t_p + t_b)$) on the zinc pickup of the weld deposit are given in Table 3. At a given pulse frequency, the increase in pulse duration was found (Table 3) to enhance the zinc pickup in weld deposit; whereas, at a given pulse frequency, the increase in pulse off time fraction was found (Table 3) to reduce the zinc pickup in the weld. The existence of zinc in the weld deposit caused precipitation of $Mg_3Zn_3Al_2$ in the matrix, as identified (Table 4) by the presence of $(Al,Zn)_{49}Mg_{32}$ under the x-ray diffraction studies. The presence of $(Al,Zn)_{49}Mg_{32}$, which is in close approximation by nature (Ref. 21) to the $Mg_3Zn_3Al_2$, has been identified and confirmed by the interplanar spacing (d-value) where, no other interfering d value is observed. The stoichiometric amount of precipitate has been found to increase with the enhancement of zinc pickup as shown in Table 4.

Microstructure

The microstructure of the multipass weld was found to consist of a mixture of coarse columnar dendritic and relatively finer dendritic regions. These two regions are largely defined by their different dendrite arm spacing and the aspect ratio of dendrite arms measured under a scanning electron microscope (SEM). It was observed that the dendrite arm spacing of the coarse columnar dendrite was

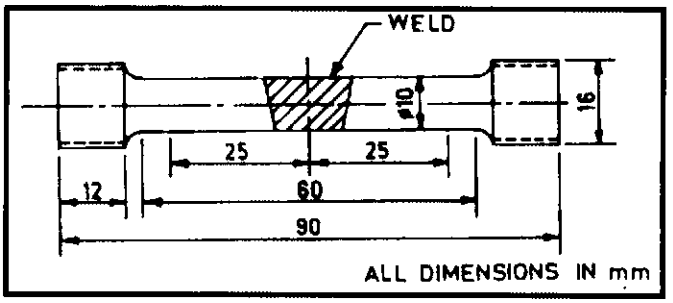

Fig. 3 — Schematic diagram of the tensile specimen.

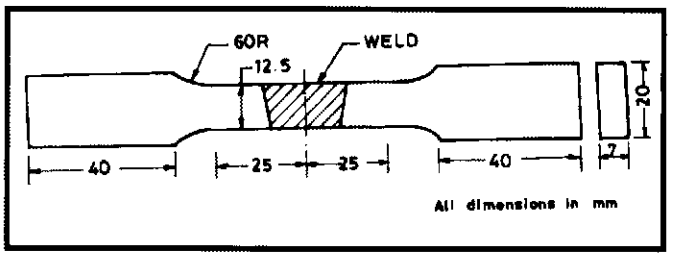

Fig. 4 — Schematic diagram of the fatigue test specimen.

Table 2 — Chemical Composition of Base Metal and Filler Metal

Material	Zn	Mg	Mn	Fe	Si	Cu	Cr	Al
Base metal (Wt-%)	4.5	1.20	0.47	0.32	0.30	0.02	0.15	Rest
Filler Metal (Wt-%)	–	4.5	0.65	—	—	—	—	Rest

Table 3 — Dilution, Zinc Content, Amount of Precipitate, Fine Dendrite Fraction and Porosity Content of the Weld Deposit at Different Welding Parameters

Specimen Designation	Dilution (%)	Zinc Pickup (Wt-%)	Amount of $(Al, Zn)_{49}$ Mg_{32} Precipitate (Wt-%)	Finer Dendrite Fraction (Area-%)	Porosity Content (Vol-%)
A	17.5	0.64	1.0539	39	2.4
B	15.5	0.60	0.9880	51	3.4
C	13	0.53	0.8563	59	2.9
D	14.5	0.56	0.9180	49	2.3
E	17.5	0.67	1.1033	60	3.0
F	15.5	0.58	0.9551	65	2.7
G	18	0.69	1.1362	56	2.1
H	19.5	0.72	1.1856	55	2.25
I	17.5	0.68	1.1198	61	1.80
J	21	0.78	1.2845	52	1.40

Table 4 — X-ray Diffraction Analysis of the Weld Bead

Sin θ	d A°	(h k l)
0.761	1.0124	(400) Al
0.659	1.169	(222) Al
0.631	1.221	(311) Al
0.538	1.431	(220) Al
0.536	1.437	(941, 853) (Al, $Zn)_{49}Mg_{32}$
0.383	2.012	(710, 550) (Al, $Zn)_{49}Mg_{32}$
0.380	2.024	(200) Al
0.333	2.310	(611, 532) (Al, $Zn)_{49}Mg_{32}$
0.330	2.338	(111) Al

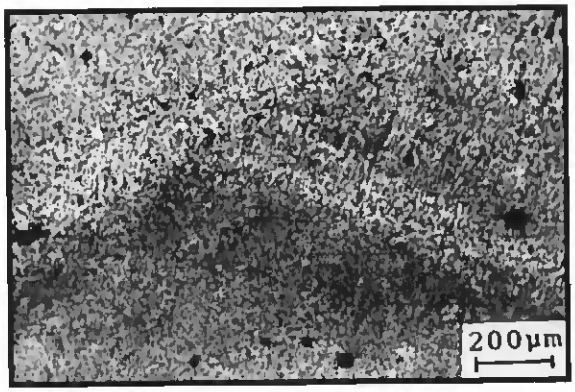

Fig. 5 — Typical microstructure of the continuous current GMA weld.

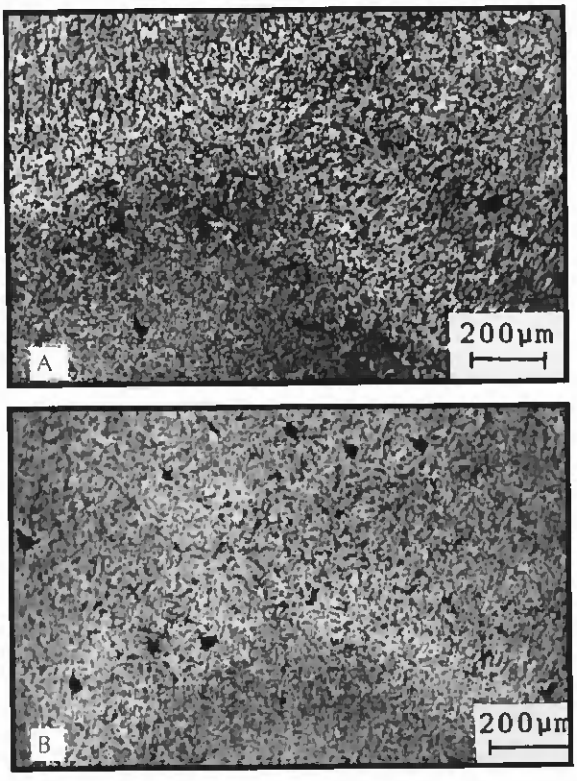

Fig. 6 — Typical microstructures of the pulsed current welds having comparatively low and high fine dendrite content.

of the order of 4.78 ±1.27 µm with an aspect ratio of 0.22 ± 0.024, where the dendrite arm spacing of the relatively finer dendrite is of the order of 1.54 ± 0.69 µm with an aspect ratio of 0.144 ± 0.020. The microstructure of the weld deposit produced by continuous current welding is presented in Fig. 5. The variation in pulse parameters has been found to affect the coarse columnar or fine dendrite content of the matrix as shown in Table 3. Typical micrographs of the pulsed current weld deposit with comparatively low and high fine dendrite content are shown in Fig. 6A and B, respectively. Table 3 shows that at a given pulse duration the increase in pulse frequency from 25 to 50 Hz enhances the fine dendrite fraction of the weld followed by a decrease with an increase in pulse frequency to 100 Hz. It is also observed that at a given pulse frequency the increase in pulse duration from 4.5 ms to 6.5 ms enhances the fine dendrite fraction of the weld followed by a decrease with an increase in pulse duration to 8.5 ms. At a given pulse frequency, a similar influence of pulse off time fraction on the fine dendrite fraction of the weld is observed as found in the case of the variation in pulse duration. However, it was observed that the pulsed current weld contained more fine dendrite in comparison to the conventional continuous current weld.

Table 5 — Tensile Properties of the Welded Joint

Pulse Frequency (Hz)	Pulse Duration (ms)	Yield Strength (N/mm^2)	Ultimate Tensile Strength (N/mm^2)	Elongation (%)
0	—	162	260	6.0
25	4.5	170.5	270	6.2
50	4.5	172	277	6.6
100	4.5	171.5	273	6.3
25	6.5	172	275	6.7
50	6.5	174	287	7.5
100	6.5	172.5	280	7.0
25	8.5	173.5	280	7.2
50	8.5	176.5	300	9.0
100	8.5	174	289	8.2

Porosity Content of the Weld Deposit

Micrographs presented in Figs. 5 and 6 show the presence of porosity in the weld prepared by both the continuous and pulsed current processes. Pores are mostly round in shape. The amount of porosity in the weld was found to vary with the change in welding parameters as depicted in Table 3. The table shows that at a given pulse frequency the increase in pulse duration, and at a given pulse duration the increase in pulse frequency, reduces the porosity content of the weld. A decrease in pulse off time fraction was found to reduce the porosity content of the weld. It may be further noted that a proper selection of pulse parameters, such as a higher pulse frequency and duration of 100 Hz and 8.5 ms, resepectively, can reduce the porosity content of the weld significantly in comparison to continuous current welds.

Tensile Properties

The influence of welding parameters on the tensile properties of the joint, such as yield strength (σ_{YZ}), tensile strength (σ_u) and elongation (e_f) are shown in Table 5. During tensile testing of the weldments, the specimens were found to fracture in the weld region. Thus, it may be assumed that the tensile and yield strengths depicted in Table 5 primarily represent the tensile and yield strengths of the weld (Refs. 8, 9). The table reveals that the use of pulsed current instead of continuous current influences the tensile properties of the weld. It is also marked that during pulsed current welding the variation in pulse parameters affects the tensile properties of the weld significantly. The change in tensile properties with the pulse parameters is primarily attributed to the porosity content, zinc pick-up and fine dendrite fraction of the weld fatigue properties.

Fatigue Properties

During fatigue testing of both the continuous and pulsed current GMA weldments, fracture occured in the weld region. However, the fatigue life of the pulsed current weld is found to vary with a change in pulse parameters. At a given pulse duration, the influence of pulse frequency on the fatigue life of the weld is shown in Fig. 7. Similarly, at a given pulse frequency, the influence of pulse off time fraction on the fatigue life of the weld joint is presented in Fig. 8. Figure 7 shows that the increase in pulse fre-

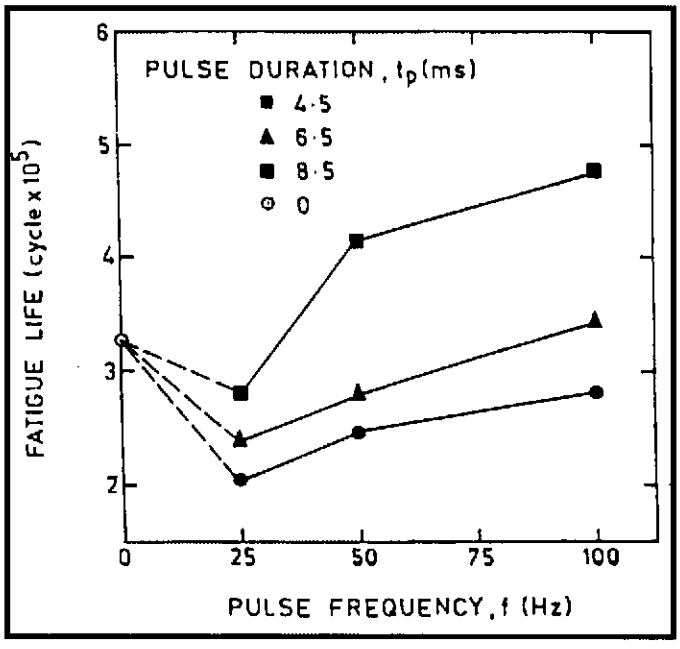

Fig. 7 — At a given pulse duration, the effect of pulse frequency on fatigue life of the weld joints.

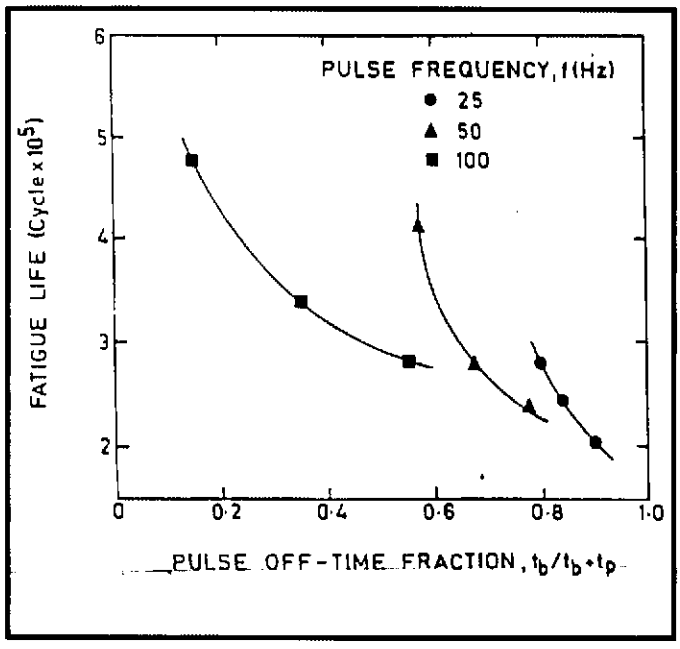

Fig. 8 — At a given pulse frequency, the effect of pulse off time fraction on fatigue life of the weld joints.

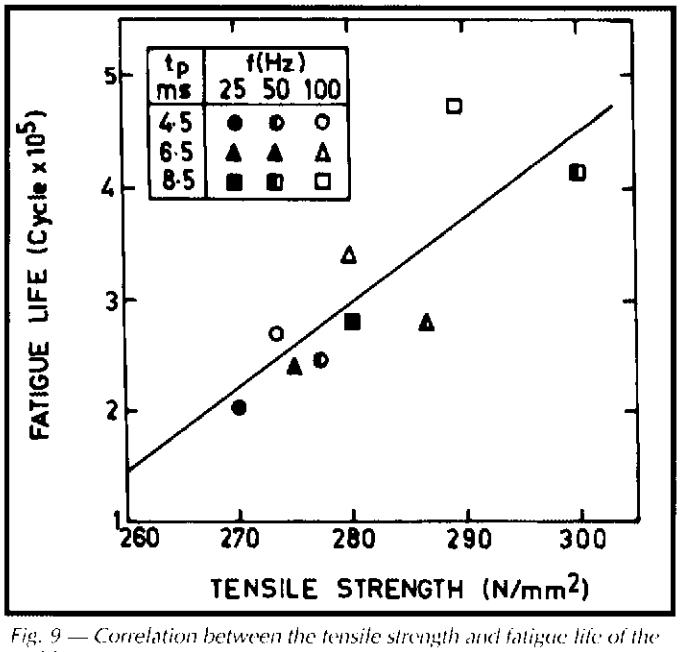

Fig. 9 — Correlation between the tensile strength and fatigue life of the weld joint.

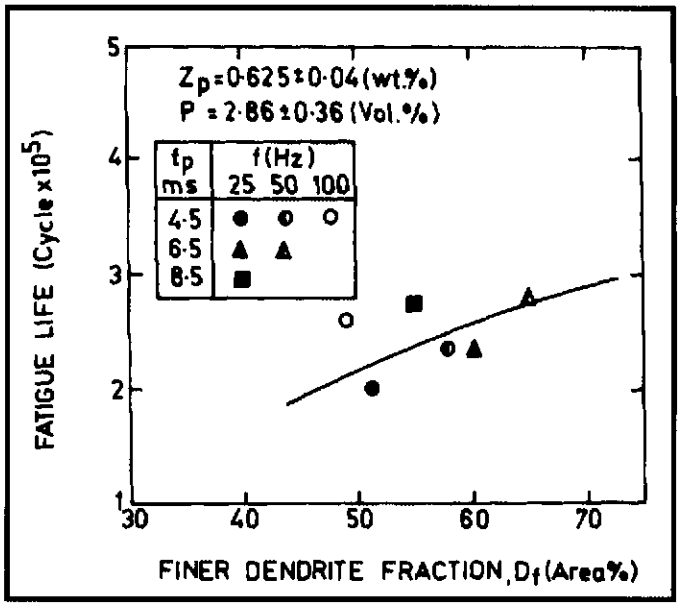

Fig. 10 — At a given zinc pickup and porosity content, the influence of fine dendrite fraction on fatigue life of the weld joints.

quency from 25 to 100 Hz improves the fatigue life of the weld significantly, especially when the pulse duration is kept at 8.5 ms. Figure 7 also shows that the increase in pulse duration from 4.5 to 8.5 ms also enhances the fatigue life of the weld significantly, especially at the pulse frequencies of 50 and 100 Hz. But, at a given pulse frequency, the increase in pulse off time fraction has been found (Fig. 8) to appreciably reduce the fatigue life of the weld. The fatigue life of the continuous and pulsed current welds presented in Fig. 7 reveals that the use of pulsed current welding at a pulse frequency of 50 Hz or more under a pulse duration of 8.5 ms improves the fatigue life of the weld over that observed in the continous current weld.

Fatigue life of a weld is primarily governed by the loading condition, its porosity content, and microstructure. In this investigation, the fatigue tests were carried out at a given mean stress (σ_m) of 80 N/mm^2. With pulsed current welding, the yield strength of the weld was found to vary insignificantly (Table 5), so during testing, the applied mean stress can be estimated as about 47% of the yield strength of the welds. Thus, in this case the fatigue life of the weld is assumed to be primarily governed by the tensile stregth, σ_u, of the weld, which varies with a change in pulse parameters — Table 5. A correlation of the fatigue life of the weld with a tensile strength (Fig. 9) having a coefficient of correlation of 79% is also verified by this report. The correlation of the fatigue life with the tensile strength of the weld is found as

$$N = 7497.22\ \sigma_u - 1800202.1 \qquad (1)$$

At a given σ_m, the increase in σ_u improves the fatigue life of the weld due to

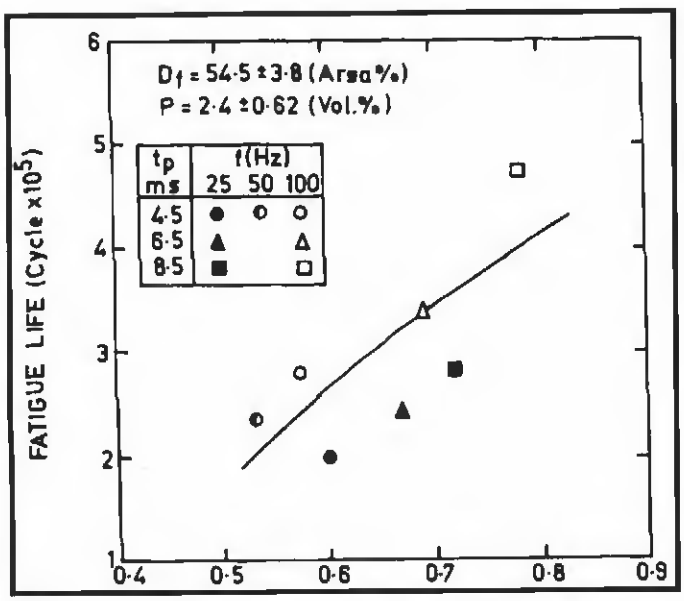

Fig. 11 — At a given fine dendrite fraction and porosity content, the influence of zinc pickup on fatigue life of the weld joints.

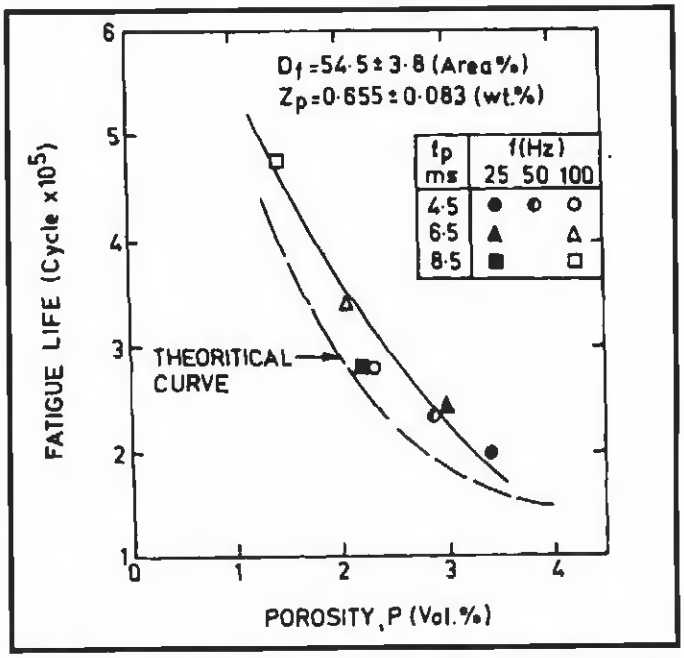

Fig. 12 — At a given zinc pickup and fine dendrite fraction the influence of porosity content on fatigue life of the weld joints.

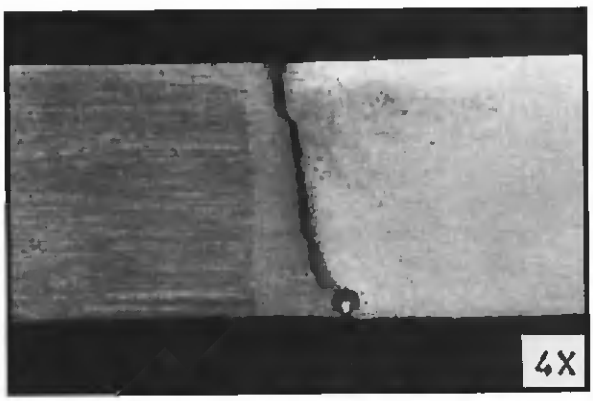

Fig. 13 — Typical macrograph of fatigue fracture of weld joint showing the presence of porosity at the surface.

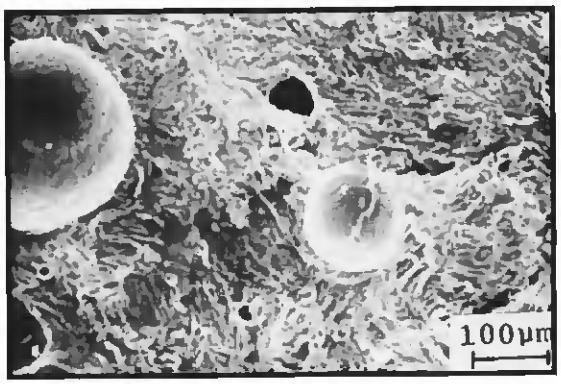

Fig. 14 — Typical fractograph of pulsed current weld shown comparatively low fatigue life.

reduction in ratio of σ_m/σ_u (Ref. 22). The tensile strength of the weld is found to be influenced by its microstructure, zinc pickup and porosity content. Thus, it is imperative to study the influence of these aspects on the fatigue life of the weld.

At a given zinc pickup and porosity content of 0.625 ± 0.04 wt-% and 2.86 ± 0.36 vol-%, respectively, the effect of weld deposit microstructure on the fatigue life of the weld is presented in Fig. 10. The microstructure of the weld deposit, defined as its fine dendrite content, D_f (area %) is correlated to its fatigue life (N cycle) as follows, having a coefficient of correlation on the order of 63%:

$$N = 225746.63 \ln D_i - 664461.2 \quad (2)$$

Figure 10 shows that the increase in fine dendrite fraction enhances the fatigue life of the weld primarily due to establishment of a homogeneous slip, reducing the local stress concentration and plastic deformation (Ref. 22). Similarly, at a given fine dendrite and porosity content of 54.5% (± 3.8% area) and 2.4% (± 0.62 vol-%), respectively, the infuence of zinc pickup (Z_p), and at a given fine dendrite content and zinc pickup of 54.5% (±3.8% area) and 0.655% (±0.083 wt-%), respectively, the influence of porosity (P) on the fatigue life of the weld is shown in Figs. 11 and 12, respectively. As previously reasoned, the increase in zinc pickup and porosity content is found to increase (Fig. 11) and decrease (Fig. 12) the fatigue life of the weld primarily due to their positive and negative influence on the tensile strength of the weld. The fatigue life of the weld is found to be correlated with the Z_p (wt-%) and P (vol-%) of the weld as given below, following the coefficients of correlation of 69% and 96%, respectively.

$$N = 504652 \ln Z_p + 523445 \quad (3)$$
$$N = 596403 - 337520 \ln P \quad (4)$$

However, regarding the influence of porosity content on the fatigue life of the weld, it may also be noted that the increase in porosity content of the weld enhances the possiblity of the presence of pores at the weld surface, which also reduces fatigue life by providing sites for crack initiation as shown in Fig. 13. The correlation of N with P presented in Fig. 12 closely approximates a theoretical line reported earlier (Ref. 9)

Typical fractographs of the welds showing comparatively low and high fa-

tigue life are shown in Figs. 14 and 15, respectively. The figures depict that the weld with a comparatively low fatigue life has a considerable amount of porosity (Fig. 14) in comparison to that observed in the weld with high fatigue life — Fig. 15. Figure 15 also shows that the fracture morphology is comparatively fine in the weld with high fatigue lifeas opposed to the weld having comparatively a low fatigue life — Fig. 14. This is in agreement to the earlier discussions, regarding occurence of a homogeneous slip in case of fine microstructure (Fig. 15) in the weld, resulting in enhancement of fatigue life.

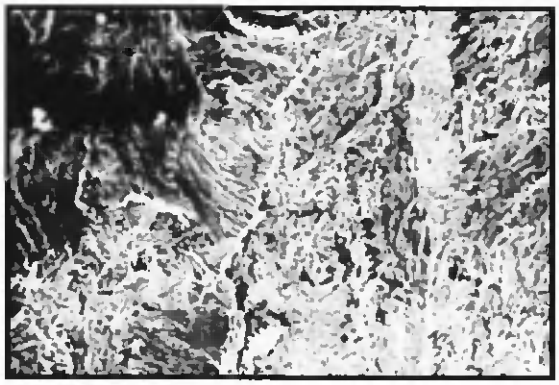

Fig. 15 — Typical fractograph of pulsed current weld shown comparatively high fatigue life.

Conclusions

During an investigation on fatigue life of the multipass pulsed current GMA welds, the joints were found to fracture in the weld. At a given pulse duration, the increase of pulse frequency from 25 to 100 Hz was found to increase the fatigue life of the weld. Similarly, at a given pulse frequency, the increase in pulse duration from 4.5 to 8.5 ms enhanced the fatigue life of the weld; whereas, the fatigue life of the weld was reduced with an increase of pulse off time fraction. During pulsed current welding, the use of a pulse frequency and duration of 50 Hz and 8.5 ms, respectively, enhanced the fatigue life of the weldment compared to that of continuous current multipass GMA welds.

The fatigue life of the weldment is governed by the microstructure, zinc pickup and porosity content of the weld. Both the increase in fine dendrite fraction and zinc pickup in the weld enhanced its fatigue life, but the increase in porosity content to 3.4 vol-% reduced the fatigue life significantly. Fatigue life of the weld is directly related to its tensile strength.

Acknowledgment

The authors thankfully acknowledge the financial assistance given by the Council of Scientific and Industrial Research (CSIR), New Delhi, Government of India, for carrying out this work.

References

1. Kent, K. G. 1970. The future of the weldable Al-Zn-Mg alloys. *Proceedings Conference on Weldable Al-Zn-Mg Alloy*, Welding Institute, Cambridge, England, pp. 110–111.

2. Baker, R. G., Scott, M. H., and Hicks, J. G. 1970. The possibilities for alloy standardization. *Proceedings Conference on Weldable Al-Zn-Mg Alloy*, Welding Institute, Cambridge, England, p. 100.

3. *Welding Handbook*. 1978. Seventh edition, Vol. 2, AWS, Miami, Fla., pp. 114–148.

4. Bonghton, P., and Lucey, J. A. 1965. The use of pulsed current to control metal transfer in welding. *British Welding Journal* 12(4): 159–166.

5. Needham, J. C., and Carter, A. W. 1965. Material transfer characteristics with pulsed current. *British Welding Journal* 12(5): 229–241.

6. Gupta, P. C., Ghosh, P. K., and Vissa, S. 1988. Influence of pulse frequency on the properties of HAZ in pulsed MIG welded Al-Zn-Mg alloy. *International Conference on Welding Technology*, University Of Roorkee, pp. 171–177.

7. Ghosh, P. K., Gupta, P. C., Gupta, S. R. and Rathi, R. 1990. Pulsed MIG welding of Al-Zn-Mg alloy. *Metallurgical Transactions JIM*, 31(8): 723–729.

8. Srikanth R. 1990. M.E. dissertation. Studies on fracture toughness properties of Al-Zn-Mg alloy weldment produced by pulsed MIG welding process. Department of Mechanical and Industrial Engineering, University of Roorkee, India.

9. Ghosh, P. K., Gupta, P. C., Gupta, S. R. and Rathi, R. 1991. Fatigue characteristics of pulsed MIG welded Al-Zn-Mg alloy. *Journal of Materials Science*, Vol. 26, pp. 6161–6170.

10. Ghosh, P. K. 1993. Pulsed current MIG welding of Al-Zn-Mg alloy — analytical modelling of thermal behaviour and correlations among pulse parameters and weld characteristics and properties. Project report, Alexandar Von Humboldt research fellowship, T. U. Berlin, Germany.

11. Potluri, N. B., Ghosh, P. K., Gupta, P. C., and Srikanth Reddy, Y. 1996. Studies on weld metal characteristics and their influence on tensile and fatigue properties of pulsed current GMA welded Al-Zn-Mg alloy. *Welding Journal* in 75(2): 62-s to 70-s.

12. Ghosh, P. K., Gupta, P. C., and Jain, N. K. 1988. Effect of pulse frequency on the weld seam properties in pulsed arc MIG welding of Al-Zn-Mg alloy. *Aluminum* 64(9): 933–935.

13. Ghosh, P. K., Sharma, V. 1991. Weld bead chemistry and its characteristics in pulsed MIG welded Al-Zn-Mg alloy. *Metallurgical Transactions JIM*, 32(2): 145–150.

14. Waszink, J. H., and Piena, M. J. 1986. Experimental investigation of drop detachment and drop velocity in GMAW. *Welding Journal*, 65(11): 289-s to 298-s.

15. Sonsino, C. M., and Dieterich, K. 1991. (Fraunhoter-Institute fur Betriebsfestig keit) Giessereiforschung, 43(4): 131–140.

16. Harisson, J. D. 1970. Fatigue behaviour and fracture toughness. *Proceedings Conference on Weldable Al-Zn-Mg Alloy*, Welding Institute, Cambridge, England, pp. 80–88.

17. Hval, M., Angleik, K., and Thaulow, C. 1992. Significance of defects in thick welded Al-Mg-Si (AA6082) aluminium extrusions. *Proceedings 5th International Conference of Aluminum Weldments* (5th INALCO 92), Munich, Germany, pp. 3.2.1–3.2.10.

18. Dehoff, R. T., and Rhines, F. N. 1968. *Quantitative Microscopy*, McGraw Hill Book Co., pp. 70–74.

19. ASTM, E466-82. 1990. *Annual Book of ASTM Standards*, pp. 540–544.

20. *Welding Alcoa Aluminium*. 1972. Aluminium Co. of America.

21. Pearson, W. B. 1967. *Handbook of Lattice Spacing and Structure of Metals*, Vol. 1.2, Pergamon Press, London, p. 574.

22. Dieter, G. E. 1976. *Mechanical Metallurgy*, Second edition, McGraw Hill Book Co., pp. 273–275.